19th Brazilian Congress of Thermal Sciences and Engineering
November 6th–10th, 2022, Bento Gonçalves - RS - Brazil

ENC-2022-0298
FINITE ELEMENT METHOD APPLIED TO DIESEL PARTICULATE FILTER FLOW

Felipe Feres Ferreira
Gustavo Rabello dos Anjos
Universidade Federal do Rio de Janeiro, COPPE / Departamento de Engenharia Mecânica
felipeferesferreira@mecanica.coppe.ufrj.br
gustavo.rabello@coppe.ufrj.br

Abstract. *Nowadays, air pollution is one of the greatest problems faced by humanity and one of its main causes is the gases present in the vehicle's exhaust. In order to mitigate these problems in diesel-fueled vehicles, it is usually used a device named Diesel Particulate Filter, also known as DPF, which is responsible for filtering the particulates contained in the exhausted air. Since currently there are very strict laws regulating the quantity of particulate which are being exhausted into the atmosphere, it is very important to study this device to ensure its performance and to make improvements possible. So, to study the flow behavior inside this device, this work aims to develop a computational code using a CFD approach. This case was modeled as a single-phase air flow inside the device and the air was modeled as an incompressible Newtonian fluid. The governing equations of the flow are the Navier-Stokes equations and, since there is a porous media inside the DPF, the Darcy-Forchheimer model is used in the Navier-Stokes equations to represent the effects of this region. The Finite Element Method (FEM) was the numerical method used, using a semi-Lagrangian method to discretize the derivative material and the Galerkin approximation to discretize the other terms in the spatial domain. After all, it is necessary to verify if the code provides results consistent with reality. In order to do that, it is simulated cases in which the results are well established in the literature, making it possible to compare code and literature results and to verify the results' consistency. This verification shows that the code is highly reliable.*

Keywords: *Finite Element Method, Diesel Particulate Filter, Darcy-Forchheimer, Semi-Lagrangian, Porous Media*

1. INTRODUCTION

It is well known that pollution is a huge problem which is causing not only environmental impact but also affecting people's health. Because of that, more and more efforts are being made to mitigate this problem with technologies being developed and optimized to reduce it. In particular, it is possible to mention air pollution as one of the main pollution problems, causing not only respiratory diseases but also the greenhouse effect. The principal cause of air pollution is the burning of fossil fuels, which mostly are made by industrial facilities and motor vehicles.

In recent years there has been an increase in the number of motor vehicles which are running around the world and, because of that, it is important to make efforts to reduce its pollutant emissions. Diesel engines, present in a lot of vehicles, have a significant contribution to the pollution problem, mainly because of the diesel exhaust gas since it contains a large amount of NO_X and particulate matter (Reşitoğlu *et al.*, 2015).

In order to mitigate these pollution problems caused by diesel engines, stringent emission regulations have been established. So, since until now the only effective way to control the emissions is using the Diesel Particulate Filter, its usage has been mandatory (Guan *et al.*, 2015).

The DPF, short for Diesel Particulate Filter, is a device used to remove the particulate matter from the diesel engine's exhausted gas. Since its usage is mandatory on diesel engine vehicles, it is very important to study it to reach lower particulate matter emissions and to make that its usage does not reduce the engine performance.

DPF works by trapping and retaining the particulate matter and by eliminating it in a safe way (Khair, 2003). There are different types of configurations for the DPF that are responsible for the trapping and retaining process. The most used one is the wall-flow type, a configuration that has a honeycomb structure with parallel channels that are plugged alternatively into one of its ends. Moreover, the channel walls are constituted by a porous material where the particulate matter is trapped (Rodríguez-Fernández *et al.*, 2017).

In Fig. 1 it is possible to see a schematic representation of the channels inside of DPF. On the left, there is a front

view of a sample of nine channels where can be seen how the plugs are arranged alternatively. It is important to note that the channels that are shown plugged are opened on the other end and the channels shown opened are plugged. Moreover, even though it is only shown nine channels, in a DPF there are a lot more of them and the choice to show only nine was made for clarity reasons.

On the right of Fig. 1, there is a section view of channels inside. In this view, it is possible to see how the trapping process occurs inside the device. The exhausted air enters the opened channels and, since the channel's end is plugged, the air is forced to pass through the porous walls to leave the device. So, it is when the air is passing through the porous wall that most particulate matter is get trapped in the wall itself.

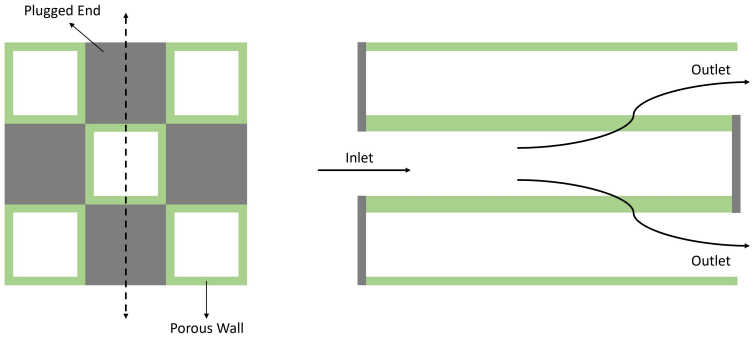

Figure 1. Schematic representation of DPF's channels.

The particulate matter trapping process can not be carried out alone, since it would cause an accumulation of it in the DPF and, therefore, a decrease in the engine performance. So, to avoid this problem, a regeneration process, which consists in safely burning the trapped particulate matter, is usually also carried out.

Looking at the trapping process, it is possible to see that the porous wall plays the main role in it and, because of that, understanding the flow behavior through it is essential to study the DPF. Actually, no special treatment would be necessary to study this flow and the traditional conservation equations would be able to describe its behavior. However, to use this traditional approach on it, it would be necessary to describe correctly the porous geometry. Then, since the porous have a very complex geometry, this description would be very difficult to do, so, modeling the effects of this region on the flow usually is the best option (Slattery, 1999).

The model which has the simplest relation between pressure and velocity is Darcy's Law. This model provides good results for cases where the inertial effects can be neglected and is presented by Eq. (1), where $\mathbf{u}$ refers to the velocity vector, K to the permeability coefficient, μ to the fluid dynamic viscosity and P to the pressure (Cimolin and Discacciati, 2013).

$$\mathbf{u} = -\frac{K}{\mu}\nabla P \tag{1}$$

Since Darcy's Law does not work well when there are inertial effects present, there is another model that provides good results when these effects are present. This is the Forchheimer equation, which is presented by Eq. (2) where ρ is the fluid density and C_F is the inertial resistance coefficient (Cimolin and Discacciati, 2013).

$$\nabla P = -\frac{\mu}{K}\mathbf{u} - \frac{\rho C_F}{\sqrt{K}}|\mathbf{u}|\mathbf{u} \tag{2}$$

Moreover, there are also some cases where the flow behavior can not be described well by either Darcy's Law or the Forchheimer equation. For these cases, usually, correction terms are added to Darcy's Law to get better results (Cimolin and Discacciati, 2013).

It is possible to say that most problems of fluid mechanics do not have an analytical solution yet. In order to solve these problems, numerical methods have been widely used to obtain approximated solutions since the recently computational capacity made it possible. This field is known as Computational Fluid Dynamics or just CFD.

Then, there have been some works that used the CFD methodology to study DPF. Piscaglia *et al.* (2009) used OpenFOAM, an open-source software that uses the Finite Volume Method, to solve the flow inside a DPF. In this work, it was used the Navier-Stokes equations for a compressible flow with the addition of Darcy and Forchheimer terms for the porous medium. In Konstandopoulos *et al.* (1999) and Deuschle *et al.* (2008) works, it was used the incompressible

Navier-Stokes equations along with Darcy and Forchheimer terms for the porous region. Besides that, the commercial code FLUENT, which is also based on the Finite Volume Method, was used to solve them. Souza (2021) developed a code in Python which uses the Finite Element Method to solve the same incompressible Navier-Stokes with Darcy and Forchheimer terms.

Sbrizzai *et al.* (2005) used the Navier-Stokes equations to describe the flow in the fluid region while in the porous region it was used the Ergun equation. In order to calculate it, it was used the Finite Volume Method applied by the commercial software Star-CD. Janiszewski and Teodorczyk (2016) also used the usual Navier-Stokes equations in the fluid domain, but in the porous domain, they used modified Navier-Stokes equations where it is taken into account the porosity and added an extra term related to the Darcy's Law.

Therefore, this works aims to develop a computational code to solve a case of a two-dimensional incompressible flow with porous media and to apply it to study the flow inside a DPF. Firstly, it was presented an introduction to the problem, showing the background of the problem and presenting information necessary to understand it. After that, it is going to be presented the equations that will describe the problem and, then, the numerical method used to solve these equations. Finally, a simulation of a DPF case will be run using the method presented, the results obtained will be discussed and, after all, the conclusions of this work will be made.

2. MATHEMATICAL MODEL

The DPF can be divided into two different regions: a porous region, which is constituted by the porous wall, and a fluid region. In the fluid region, the flow behavior can be described by mass and momentum conservation equations. So, accordingly to Batchelor (2000), for an incompressible flow, the mass and momentum conservation equations are presented, respectively, by Eq. (3) and Eq. (4), where $\mathbf{u}$ is the velocity vector, P is pressure, ρ is the fluid density, μ is the dynamic viscosity and $\mathbf{g}$ is the gravity vector.

$$\nabla \cdot \mathbf{u} = 0 \tag{3}$$

$$\rho \frac{D\mathbf{u}}{Dt} = -\nabla P + \mu \nabla^2 \mathbf{u} + \rho \mathbf{g} \tag{4}$$

The flow inside the porous domain could be described by Eq. (1) or Eq. (2) along with Eq. (3), since the mass conservation equation is also valid in this region. This approach would make it necessary to set coupling conditions in the interface between the fluid and porous domains. However, this approach could be problematic because of the difference in the nature of the equations used in each domain.

There is another approach that can handle this problem in a better way. In this approach Eq. (4) is modified by adding two penalization terms related to Eq. (2) in such a way that the new equation can be used in both domains by changing the penalty coefficient value. This equation is presented by Eq. (5), where K is the permeability, C_F is the inertial resistance coefficient and ε is the penalty coefficient which values are $\varepsilon = 0$ in the fluid domain and $\varepsilon = 1$ in the porous domain (Cimolin and Discacciati, 2013).

$$\rho \frac{D\mathbf{u}}{Dt} = -\nabla P + \mu \nabla^2 \mathbf{u} + \rho \mathbf{g} - \left(\frac{\mu}{K} \mathbf{u} + \frac{\rho C_F}{\sqrt{K}} |\mathbf{u}| \mathbf{u} \right) \varepsilon \tag{5}$$

Then, Eq. (3) and Eq. (5) are the governing equations that will be used to describe the flow behavior inside the DPF in this work. Moreover, in order to obtain their dimensionless form, it is introduced the dimensionless form of the variables first. So, being L_c and U_c the flow characteristic length and velocity, respectively, the variable dimensionless form are presented by Eq. (6), where $\mathbf{x}$ is the position vector, $\mathbf{u}$ is the velocity vector, t is the time, P is the pressure, ρ is the density, $\mathbf{g}$ is the gravity vector and the symbol $'$ refers to the dimensionless form.

$$\mathbf{x}' = \frac{\mathbf{x}}{L_c}, \qquad \mathbf{u}' = \frac{\mathbf{u}}{U_c}, \qquad t' = \frac{U_c}{L_c} t, \qquad P' = \frac{P}{\rho U_c}, \qquad \mathbf{g}' = \frac{\mathbf{g}}{|\mathbf{g}|} \tag{6}$$

Then, using the dimensionless parameters, it is possible to get the dimensionless form of the governing equations Eq. (3) and Eq. (5) presented, respectively, by Eq. (7) and Eq. (8)

$$\nabla \cdot \mathbf{u}' = 0 \tag{7}$$

$$\frac{D\mathbf{u}'}{Dt'} = -\nabla P' + \frac{1}{Re} \nabla^2 \mathbf{u}' + \frac{1}{Fr^2} \mathbf{g}' - \left(Di_1 \mathbf{u}' + Di_2 |\mathbf{u}'| \mathbf{u}' \right) \varepsilon \tag{8}$$

Where Re is the Reynolds number, Fr is the Froude number and Di_1 and Di_2 are also dimensionless groups. All of them are defined as presented by Eq. (9).

$$Re = \frac{\rho U_c L_c}{\mu}, \qquad Fr = \frac{U_c}{\sqrt{|\mathbf{g}| L_c}}, \qquad Di_1 = \frac{\mu L_c}{\rho K U_c} \qquad Di_2 = \frac{L_c C_F}{\sqrt{K}} \tag{9}$$

3. FINITE ELEMENT METHOD

The method that is used in this work to obtain an approximated solution for the governing equations is the Finite Element Method. In this method the problem domain is sub-divided into a finite number of sub-regions, usually called elements, and, then, the weak form of the equations is integrated over each element (Ferzig and Peric, 2002).

3.1 Weak form

The main steps of the method are to obtain the weak or variational form of the governing equations and to use some function to obtain an approximate solution for them (Hughes, 1987). Firstly, it is necessary to establish the weak formulation of the problem. So, after operating Eq. (7) and Eq. (8) with weighting functions and applying integration by parts and divergence theorem, the weak form of the governing equations are obtained, which are presented by Eq. (10) and Eq. (11) where q and $\mathbf{w}$ are weighting function, Ω refers to the problem domain and Γ to the boundaries of the domain.

$$\int_\Omega q(\nabla \cdot \mathbf{u}')d\Omega = 0 \tag{10}$$

$$\begin{aligned}\int_\Omega \mathbf{w} \cdot \frac{D\mathbf{u}'}{Dt'}d\Omega &= \int_\Omega P'(\nabla \cdot \mathbf{w})d\Omega - \int_\Gamma P'\mathbf{w} \cdot \mathbf{n}d\Gamma + \frac{1}{Re}\left(-\int_\Omega \nabla\mathbf{w}^T : \nabla\mathbf{u}'d\Omega + \int_\Gamma \mathbf{w} \cdot \nabla\mathbf{u}' \cdot \mathbf{n}d\Gamma\right) + \\ &+ \frac{1}{Fr^2}\int_\Omega \mathbf{w} \cdot \mathbf{g}'d\Omega - \int_\Omega \mathbf{w} \cdot (Di_1\mathbf{u}' + Di_2|\mathbf{u}'|\mathbf{u}')\varepsilon d\Omega\end{aligned} \tag{11}$$

In this work, since the boundary conditions that are applied are Dirichlet, homogeneous Neumann, and a null prescribed pressure, the terms in Eq. (11) related to the boundaries of the domain are going to be null. Moreover, the porous term will be null in the fluid domain and, because of that, it can be integrated only over the porous domain. So, Eq. (11) can be simplified to Eq. (12), where Ω_p refers to the porous domain.

$$\int_\Omega \mathbf{w} \cdot \frac{D\mathbf{u}'}{Dt'}d\Omega = \int_\Omega P'(\nabla \cdot \mathbf{w})d\Omega - \frac{1}{Re}\int_\Omega \nabla\mathbf{w}^T : \nabla\mathbf{u}'d\Omega + \frac{1}{Fr^2}\int_\Omega \mathbf{w} \cdot \mathbf{g}'d\Omega - \int_{\Omega_p}(Di_1 + Di_2|\mathbf{u}'|)\mathbf{w} \cdot \mathbf{u}'d\Omega_p \tag{12}$$

Before start the discretization process of Eq. (10) and Eq. (12), the equations are rewritten for clarity reasons. Since the problem studied in this work is 2D, it is possible to represented the vectors as $\mathbf{x}' = [x_1' \ x_2']^T$, $\mathbf{u}' = [u_1' \ u_2']^T$, $\mathbf{g}' = [g_1' \ g_2']^T$ and $\mathbf{w} = [w_1 \ w_2]^T$. So, the weak formulation of the governing equations can be written as presented by Eq. (13), Eq. (14) and Eq. (15).

$$\int_\Omega q\frac{\partial u_1'}{\partial x_1'}d\Omega + \int_\Omega q\frac{\partial u_2'}{\partial x_2'}d\Omega = 0 \tag{13}$$

$$\begin{aligned}\int_\Omega w_1\frac{Du_1'}{Dt'}d\Omega &= \int_\Omega P'\frac{\partial w_1}{\partial x_1'}d\Omega - \frac{1}{Re}\int_\Omega\left(\frac{\partial w_1}{\partial x_1'}\frac{\partial u_1'}{\partial x_1'} + \frac{\partial w_1}{\partial x_2'}\frac{\partial u_1'}{\partial x_2'}\right)d\Omega + \\ &+ \frac{1}{Fr^2}\int_\Omega w_1 g_1'd\Omega - \int_{\Omega_p}(Di_1 + Di_2|\mathbf{u}'|)w_1u_1'd\Omega_p\end{aligned} \tag{14}$$

$$\begin{aligned}\int_\Omega w_2\frac{Du_2'}{Dt'}d\Omega &= \int_\Omega P'\frac{\partial w_2}{\partial x_2'}d\Omega - \frac{1}{Re}\int_\Omega\left(\frac{\partial w_2}{\partial x_1'}\frac{\partial u_2'}{\partial x_1'} + \frac{\partial w_2}{\partial x_2'}\frac{\partial u_2'}{\partial x_2'}\right)d\Omega + \\ &+ \frac{1}{Fr^2}\int_\Omega w_2 g_2'd\Omega - \int_{\Omega_p}(Di_1 + Di_2|\mathbf{u}'|)w_2u_2'd\Omega_p\end{aligned} \tag{15}$$

3.2 Galerkin method

After the establishment of the weak formulation of the governing equation, it is necessary to discretize it. So, the Galerkin method is used to discretize the terms in the spatial domain while the temporal term still is treated as continuous. The Galerkin method consists in approximating continuous variables to a discrete representation by using interpolation function (Hughes, 1987). So, considering NV the number of velocity nodes and NP the number of pressure nodes, the variables and weighting functions can be approximated for each element as presented by the following equations:

$$u_1' = \sum_{i=1}^{NV} N_iu_{1i}, \quad u_2' = \sum_{i=1}^{NV} N_iu_{2i}, \quad P' = \sum_{i=1}^{NP} L_iP_i, \quad q = \sum_{i=1}^{NP} L_iq_i, \quad w_1 = \sum_{i=1}^{NV} N_iw_{1i}, \quad w_2 = \sum_{i=1}^{NV} N_jw_{2i} \tag{16}$$

Then, substituting Eq. (16) in Eq. (13), Eq. (14) and Eq. (15), a linear system is obtained for all elements as presented by Eq. (17), Eq. (18) and Eq. (19) where NE is the number of elements.

$$\sum_{e=1}^{NE}\left(\int_{\Omega^e}\sum_{i=1}^{NP}\sum_{j=1}^{NV}L_i\frac{\partial N_j}{\partial x_1'}u_{1j}d\Omega+\int_{\Omega^e}\sum_{i=1}^{NP}\sum_{j=1}^{NV}L_i\frac{\partial N_j}{\partial x_1'}u_{2j}d\Omega\right)=0 \tag{17}$$

$$\sum_{e=1}^{NE}\left(\int_{\Omega^e}\sum_{i=1}^{NV}\sum_{j=1}^{NV}N_iN_j\frac{Du_{1j}}{Dt'}d\Omega+\frac{1}{Re}\int_{\Omega^e}\sum_{i=1}^{NV}\sum_{j=1}^{NV}\left(\frac{\partial N_i}{\partial x_1'}\frac{\partial N_j}{\partial x_1'}+\frac{\partial N_i}{\partial x_2'}\frac{\partial N_j}{\partial x_2'}\right)u_{1j}d\Omega+\int_{\Omega_p^e}\sum_{i=1}^{NV}\sum_{j=1}^{NV}(Di_1+\right. \tag{18}$$
$$\left.+Di_2|\mathbf{u}|_j)N_iN_ju_{1j}d\Omega_p-\int_{\Omega^e}\sum_{i=1}^{NV}\sum_{j=1}^{NP}\frac{\partial N_i}{\partial x_1'}L_jP_j\right)=\sum_{e=1}^{NE}\frac{1}{Fr^2}\int_{\Omega^e}\sum_{i=1}^{NV}\sum_{j=1}^{NV}N_iN_jg_1d\Omega$$

$$\sum_{e=1}^{NE}\left(\int_{\Omega^e}\sum_{i=1}^{NV}\sum_{j=1}^{NV}N_iN_j\frac{Du_{2j}}{Dt'}d\Omega+\frac{1}{Re}\int_{\Omega^e}\sum_{i=1}^{NV}\sum_{j=1}^{NV}\left(\frac{\partial N_i}{\partial x_1'}\frac{\partial N_j}{\partial x_1'}+\frac{\partial N_i}{\partial x_2'}\frac{\partial N_j}{\partial x_2'}\right)u_{2j}d\Omega+\int_{\Omega_p^e}\sum_{i=1}^{NV}\sum_{j=1}^{NV}(Di_1+\right. \tag{19}$$
$$\left.+Di_2|\mathbf{u}|_j)N_iN_ju_{2j}d\Omega_p-\int_{\Omega^e}\sum_{i=1}^{NV}\sum_{j=1}^{NP}\frac{\partial N_i}{\partial x_2'}L_jP_j\right)=\sum_{e=1}^{NE}\frac{1}{Fr^2}\int_{\Omega^e}\sum_{i=1}^{NV}\sum_{j=1}^{NV}N_iN_jg_2d\Omega$$

This linear system can be represented by matrices and vectors where $\{u_1\}$ is the vector containing the dimensionless velocity in x_1 direction value at all nodes, $\{u_2\}$ contains the velocity in x_2 direction, $\{p\}$ the pressure and $\{g_1\}$ and $\{g_2\}$ the gravity component in x_1 and x_2, respectively.

$$[D_x]\{u_1\}+[D_y]\{u_2\}=0 \tag{20}$$

$$[M]\frac{D\{u_1\}}{Dt'}+\left(\frac{1}{Re}[K]+(Di_1[I]+Di_2[U])[M_P]\right)\{u_1\}-[G_x]\{p\}=\frac{1}{Fr^2}[M]\{g_1\} \tag{21}$$

$$[M]\frac{D\{u_2\}}{Dt'}+\left(\frac{1}{Re}[K]+(Di_1[I]+Di_2[U])[M_P]\right)\{u_2\}-[G_y]\{p\}=\frac{1}{Fr^2}[M]\{g_2\} \tag{22}$$

Moreover, $[K]$ is the stiffness matrix, $[G_x]$ and $[G_y]$ are parts of the gradient matrix related to, respectively, x_1 and x_2 direction and $[M]$ is the mass matrix (Dos Anjos, 2012). Moreover, $[D_x]=[G_x]^T$, $[D_y]=[G_y]^T$, $[I]$ is the identity matrix, $[U]$ is a diagonal matrix with containing the value of the velocity module at each node and $[M_P]$ is equal to $[M]$ in the matrix components related to the elements which are in the porous domain while the matrix components related to elements in the fluid domain are equal to zero.

3.3 Semi-lagrangian method

In order to discretize the remaining temporal term, it is used the Semi-Lagrangian Method. This method is based on the Lagrangian coordinates, which describe the fluid flow by tracking the points along their trajectory. However, a pure Lagrangian approach where all computational nodes' trajectories would be tracked could bring disadvantages and, to avoid it, the semi-Lagrangian approach works by tracking them only until the last time step, re-initializing the mesh at each time step (Dos Anjos, 2012).

So, a material derivative can be discretized by this method using an implicit first-order scheme as presented by the following equation where α is some random variable, Δt is the time between each step, and the subscript d means departed, which refers to the previous position of that point.

$$\frac{D\alpha}{Dt}=\frac{\alpha^{n+1}-\alpha_d^n}{\Delta t} \tag{23}$$

Then, it is still necessary to find where the point was in the last time step to obtain α_d^n. This point, presented as $\mathbf{x_d}$, can be calculated by the following equation, where x^{n+1} is the current mesh nodes position.

$$\mathbf{x_d^n}=\mathbf{x^{n+1}}-\mathbf{u^n}\Delta t \tag{24}$$

After finding the departed position of the computational node, a mapping is done in the mesh, looking for the element which contains the departed position, and, after that, an interpolation of the α values in the element is done to calculate α_d^n.

So, after applying this method on Eq. (21) and Eq. (22), it is obtained the following equations that are going to be used to solve the problem along with equation Eq. (20).

$$\left([M] + \frac{1}{Re}[K] + (Di_1[I] + Di_2[U])[M_P]\right)\{u_1\}^{n+1} + [G_x]\{p\}^{n+1} = \frac{1}{\Delta t}[M]\{u_{1d}\}^n + \frac{1}{Fr^2}[M]\{g_1\} \tag{25}$$

$$\left([M] + \frac{1}{Re}[K] + (Di_1[I] + Di_2[U])[M_P]\right)\{u_2\}^{n+1} + [G_y]\{p\}^{n+1} = \frac{1}{\Delta t}[M]\{u_{2d}\}^n + \frac{1}{Fr^2}[M]\{g_2\} \tag{26}$$

4. CASE SET UP

A code was developed in Python using the presented method to be used to simulate the flow inside a DPF. So, to model the case, the following hypotheses were adopted: incompressible flow, laminar, constant temperature and two-dimensional flow. Moreover, since the DPF channels are disposed of in a regularly spaced arrangement, the flow can be studied by modelling the problem as half of a channel where the air goes into and half of a channel where the air goes out by using symmetry conditions.

The DPF model used in this work is presented by Fig. 2, where it is possible to see that in addition to the DPF itself, it is also modelled the region upstream and downstream of the device. This is necessary since the boundary conditions in the DPF inlet and outlet can not be set. So, these regions must be modelled, making it possible to set a constant velocity condition far upstream of the DPF and far downstream null pressure and fully developed flow conditions.

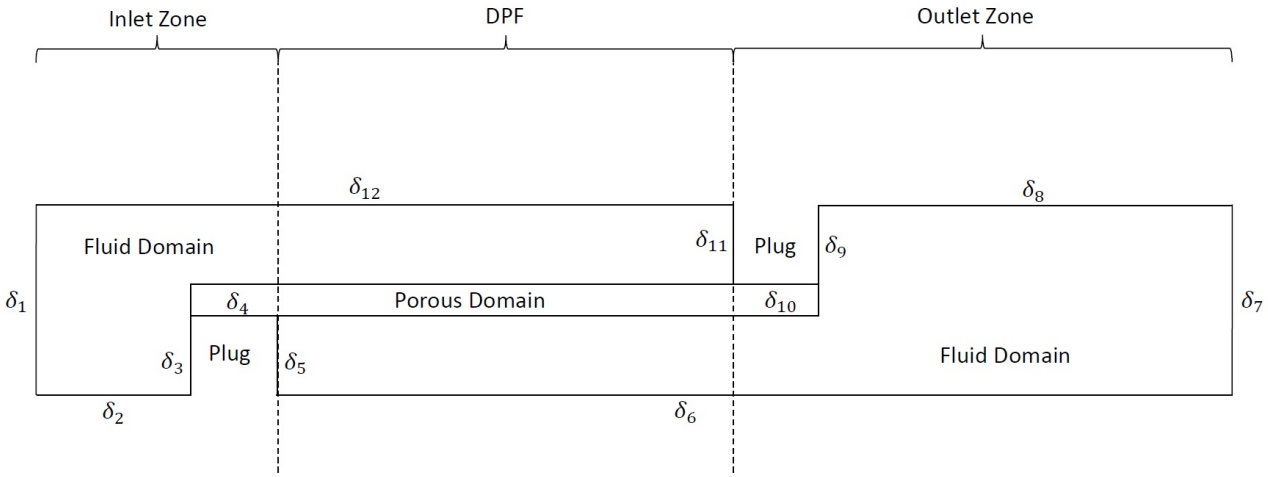

Figure 2. Model used to simulate the flow inside the DPF.

Moreover, the boundaries of the problem model are named in Fig. 2 and their definition is presented by Tab. 1.

Table 1. Mathematical definition of the problem boundary conditions.

Type	Boundaries	Velocity in x_1 direction	Velocity in x_2 direction	Pressure
Inlet	δ_1	$u_1' = 1$	$u_2' = 0$	$\frac{\partial P'}{\partial x_1'} = 0$
Symmetry	δ_2, δ_6, δ_8, δ_{12}	$\frac{\partial u_1'}{\partial x_2'} = 0$	$u_2' = 0$	$\frac{\partial P'}{\partial x_2'} = 0$
Wall	δ_3, δ_4, δ_5, δ_9, δ_{10}, δ_{11}	$u_1' = 0$	$u_2' = 0$	$\frac{\partial P'}{\partial x_1'} = 0$
Outlet	δ_7	$\frac{\partial u_1'}{\partial x_1'} = 0$	$\frac{\partial u_2'}{\partial x_1'} = 0$	$P' = 0$

The flow parameters which are adopted for this simulation are based on the work of Konstandopoulos *et al.* (1999) and they are presented by Tab. 2. Moreover, to use the dimensionless form, it is adopted that the inlet velocity is the characteristic velocity and the channel width is the characteristic length. Therefore, it is possible to relate the variables with their dimensionless form and to obtain the dimensionless groups which are present in the governing equation, especially the Reynolds number, which value is about 1000, indicating that the flow is laminar.

Finally, it is still necessary to obtain a computational mesh to run the simulation. The choice of the element which will be used is very important, since, in fluid dynamics, the element is responsible for coupling the velocity and pressure and must satisfy the Ladyzhenskaya-Babouska-Brezzi (LBB) stability condition (Dos Anjos, 2012). The element that is used in this work is the MINI element, which is from the Taylor-Hood family and satisfies the LBB condition. This element is the simplest triangular element and consists of a triangle where there are three pressure nodes located at the vertices and four velocity nodes located not only in the vertices but also in the element's centroid (Souza, 2021).

Table 2. Flow parameters.

Parameter	Value
Inlet Velocity (m/s)	24.8
Density (kg/m^3)	0.54
Dynamic Viscosity (Pa.s)	2.97 x 10^{-5}
Permeability (m^2)	2 x 10^{-13}
Inertial Resistance Coefficient (-)	223.1
Channel Width (mm)	2.11
Channel Length (mm)	304.8
Porous Wall Thickness (mm)	0.432

5. RESULTS AND DISCUSSION

The simulation was carried out using a mesh with 296434 elements, 154501 pressure nodes, and 450935 velocity nodes. The mesh was obtained using the software Gmsh and a self-developed Python code was used to add a centroid node in the elements of the mesh generated by Gmsh. The mesh is presented by Fig. 3 and Fig. 4 in detail for, respectively, the inlet and outlet of the DPF for clarity reasons.

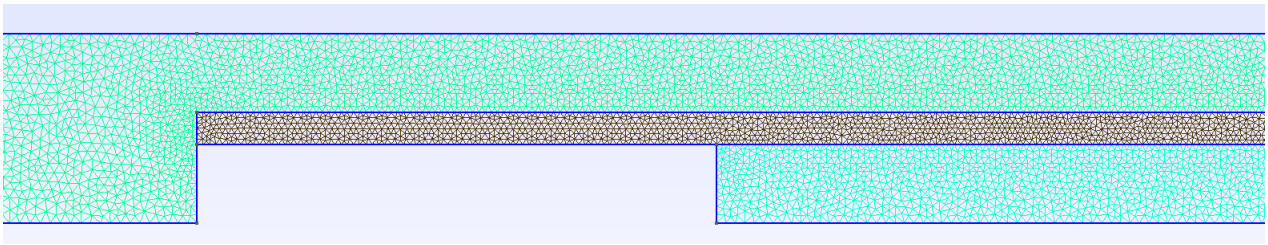

Figure 3. Mesh in the DPF inlet.

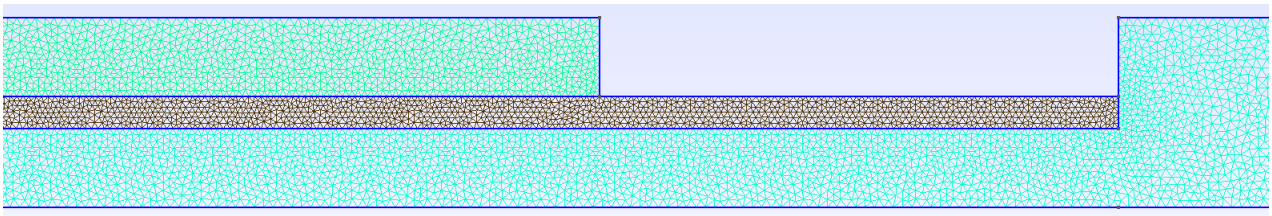

Figure 4. Mesh in the DPF outlet.

Then, the results obtained in this simulation for velocity in the x_1 direction are presented by the following figures. Since the DPF has a very long geometry, it would be difficult to show the results along all DPF clearly in one image. So, the results are shown in the DPF's inlet and outlet, respectively, by Fig. 5 and Fig. 6 with a scale of -1.2 to 3.77, represented, respectively, by dark blue and dark red colors.

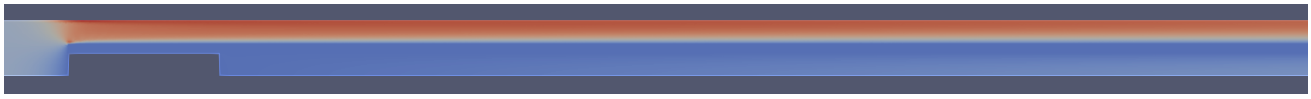

Figure 5. Velocity in x_1 direction at the inlet of DPF.

Figure 6. Velocity in x_1 direction at the outlet of DPF.

Moreover, the results were compared considering the work of Konstandopoulos *et al.* (1999) as a reference to validate the presented method. In Fig. 7 it is presented the results of the axial velocity divided by the velocity at the DPF's inlet in the inlet and outlet channels were obtained by this work and by the reference work. Furthermore, looking at the figure, it is possible to see a good agreement between this work and the reference results.

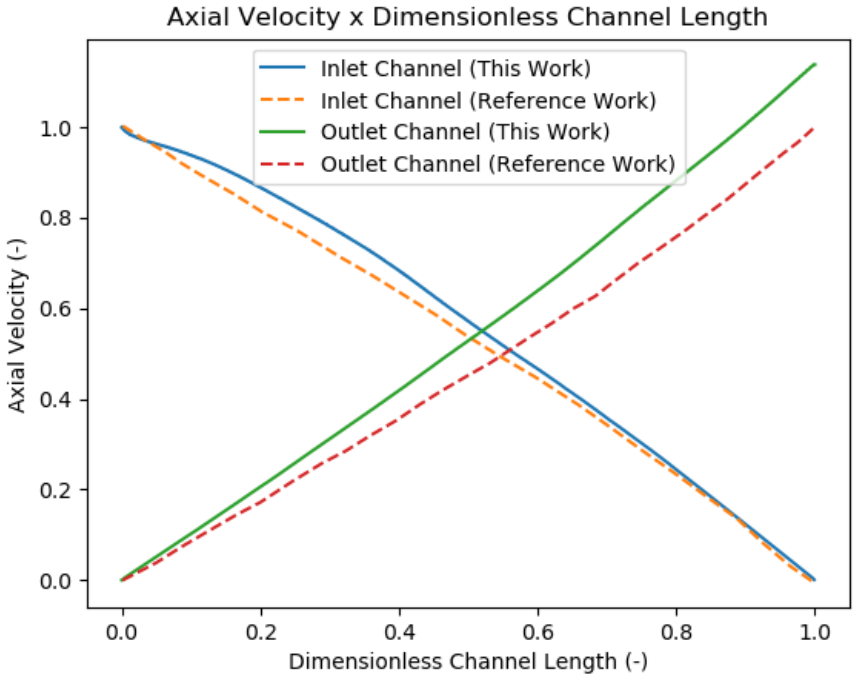

Figure 7. Axial velocity divided by the DPF's inlet velocity along inlet and outlet channels.

In Fig. 8 it is shown the velocity in the porous wall, called wall velocity, obtained in this work and the reference work. First of all, it is important to state that for this work results to be compatible with the reference work results, the dimensionless wall velocity presented is defined as presented by Eq. (27), where u_w is the wall velocity, L is the channel length, W is the channel width and U_{in} is the velocity at DPF's inlet.

$$u_w = \frac{4L}{WU_{in}}|u_2'| \tag{27}$$

Moreover, it can be observed that the wall velocity profile along the DPF of both works are similar, even though this work's wall velocity profile has higher values than the reference. This difference can be explained by Fig. 7, since it shows that, despite the good agreement between this work and the reference results, this work results have higher values along all the channels and that implies, accordingly to the mass conservation principle, in a higher mass flux through the porous wall and, therefore, in greater wall velocity.

6. CONCLUSION

In this work, it was presented a great mathematical basis to develop an approach to obtain approximated solutions for two-dimensional laminar flows with porous regions and, especially, to simulate a flow inside a DPF. Moreover, this approach was used to simulate a DPF case, comparing the results in this work with the literature results.

After comparing the results, it was observed a good agreement in the results obtained for the axial velocity at inlet and outlet channels. Besides that, despite the agreement, a trend of higher axial velocities was observed in the results obtained by this work and that might explains the fact that the wall velocity results of this work are a bit higher than the reference results.

Furthermore, the presented method seems to be reliable, considering the good mathematical basis, the consolidated numerical method which was used, and the results obtained which seem to be coherent and show a good agreement with the literature. Finally, some improvements and adaptations are recommended to be done in the future: adaptation of this method to a three-dimensional case, use of other elements type, the inclusion of solid particles in the flow turning the case into a multi-phase case, and the use of turbulence models.

7. ACKNOWLEDGEMENTS

I wish to acknowledge Agência Nacional de Petróleo (ANP) and FAPERJ for the support given to this research.

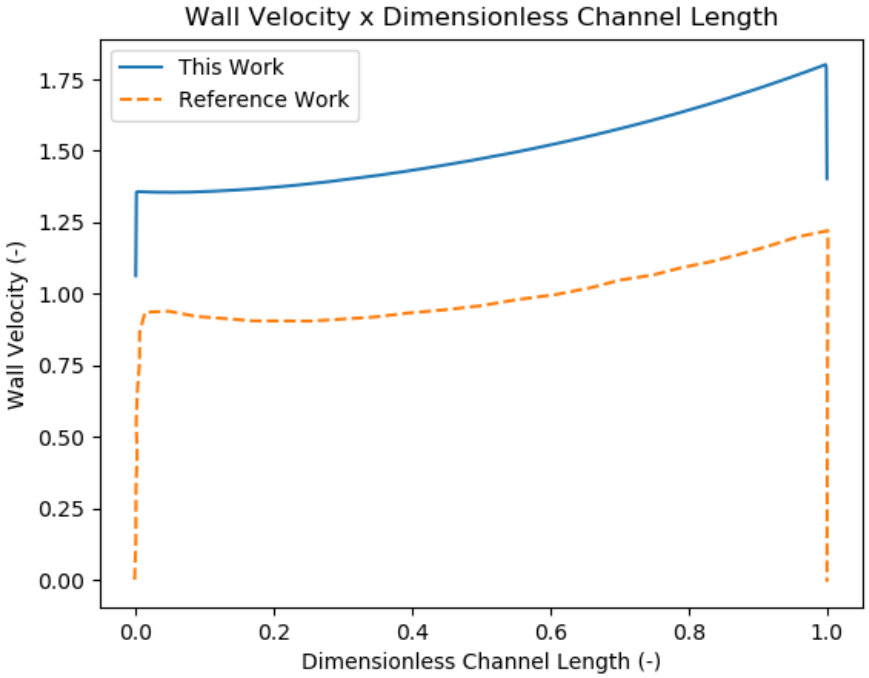

Figure 8. Velocity in the porous wall along the DPF.

8. REFERENCES

Batchelor, G.K., 2000. *An Introduction to Fluid Dynamics*. Cambridge University Press, USA, 1st edition.

Cimolin, F. and Discacciati, M., 2013. "Navier–stokes/forchheimer models for filtration through porous media". *Applied Numerical Mathematics*, Vol. 72, pp. 205–224.

Deuschle, T., Janoske, U. and Piesche, M., 2008. "A cfd-model describing filtration, regeneration and deposit rearrangement effects in gas filter systems". *Chemical Engineering Journal*, Vol. 135, pp. 49–55.

Dos Anjos, G.R., 2012. *A 3D ALE Finite Element Method for Two-Phase Flows with Phase Change*. Ph.D. thesis, École Polytechnique Fédérale de Lausanne, Lausanne, Suisse.

Ferzig, J.H. and Peric, M., 2002. *Computational Methods for Fluid Dynamics*. Springer-Verlag, New York, 3rd edition.

Guan, B., Zhan, R., Lin, H. and Huang, Z., 2015. "Review of the state-of-the-art of exhaust particulate filter technology in internal combustion engines". *Journal of Environmental Management*, Vol. 154, pp. 225–258.

Hughes, T.J.R., 1987. *The Finite Element Method: Linear Static and Dynamic Finite Element Analysis*. Prentice-Hall, Inc., USA, 1st edition.

Janiszewski, A. and Teodorczyk, A., 2016. "Cfd modeling of the regeneration process in diesel particulate filter using fluent". *Journal of KONES Powertrain and Transport*, Vol. 13, pp. 109–118.

Khair, M.K., 2003. "A review of diesel particulate filter technologies". SAE Technical Paper 2003-01-2303.

Konstandopoulos, A., Skaperdas, V., Warren, J. and Allanson, R., 1999. "Optimized filter design and selection criteria for continuously regenerating diesel particulate traps". SAE Technical Paper 1999-01-0468.

Piscaglia, F., Montorfano, A. and Onorati, A., 2009. "Development of a multi-dimensional parallel solver for full-scale dpf modeling in openfoam". SAE Technical Paper 2009-01-1965.

Reşitoğlu, I.A., Altinişik, K. and Keskin, A., 2015. "The pollutant emissions from diesel-engine vehicles and exhaust aftertreatment systems". *Clean Technologies and Environmental Policy*, Vol. 17, pp. 15–27.

Rodríguez-Fernández, J., Lapuerta, M. and Sánchez-Valdepeñas, J., 2017. "Regeneration of diesel particulate filters: Effect of renewable fuels". *Renewable Energy*, Vol. 104, pp. 30–39.

Sbrizzai, F., Faraldi, P. and Soldati, A., 2005. "Appraisal of three-dimensional numerical simulation for sub-micron particle deposition in a micro-porous ceramic filter". *Chemical Engineering Science*, Vol. 60, pp. 6551–6563.

Slattery, J.C., 1999. *Advanced Transport Phenomena*. Cambridge University Press, USA, 1st edition.

Souza, J.P.I.D., 2021. *Particle-Laden Multiphase Flows: A Finite Element Analysis on Biofuel Particle Emissions*. Master's thesis, Universidade Federal do Rio de Janeiro, Rio de Janeiro, Brasil.

9. RESPONSIBILITY NOTICE

The authors are solely responsible for the printed material included in this paper.